Theory of Overlithiation Reaction in $LiMO_2$ Battery Electrodes

R. Benedek,* J. Vaughey, and M. M. Thackeray

Electrochemical Technology Program, Chemical Engineering Division, Argonne National Laboratory, Argonne, Illinois 60439

Received August 17, 2005. Revised Manuscript Received December 29, 2005

Layered compounds with composition Li_xMO_2 and structure $R\bar{3}m$, in which M is a first-row transition metal or a combination of transition (and possibly nontransition) metals, are attractive materials for lithium-battery cathodes. For most choices of M, lithiation beyond $x = 1$ results in either decomposition or transformation to a nonlayered structure. In this article, we present first-principles calculations, on the basis of the GGA+U method, to compare addition, decomposition (with metal oxide and lithia as products), and displacement (with metal and lithia as products) reactions when an additional Li is added to $LiMO_2$. We consider M = Mn, Co, and Ni, as well as equiatomic binary mixtures of these elements. Although the displacement reaction is energetically (or thermodynamically) favored, the addition and decomposition reactions are apparently more favored kinetically, as it is the latter that are observed experimentally. The ratio of the open-circuit cell voltage to the magnitude of the reaction energy, $V_0/\Delta E_r$, is higher for systems such as $M = Mn_{0.5}Ni_{0.5}$, for which an addition reaction occurs, than for those such as M = Co, which undergoes decomposition.

Introduction

Layered O3 compounds[1] with symmetry $R\bar{3}m$ and composition Li_xMO_2 are a primary focus of lithium-battery materials research.[2] Recent attention has been given to systems with two or three transition-metal components, particularly Mn, Co, and Ni, on the transition-metal (M) sublattice.[3−9] Lithium doping on the transition-metal sublattice[10] is another strategy under investigation.

Relatively little attention has been given to the reactions undergone by these layered compounds upon discharge (relative to the Li metal) or lithiation beyond the stoichiometric value of a single Li atom per formula unit. Overlithiation to form Li_2MO_2 occurs, for example, for $M = Mn_{0.5}Ni_{0.5}$,[11] but apparently not for M = Co.[12] Li_2MnO_2 adopts a hexagonal structure,[13] but its formation by the lithiation of monoclinic $LiMnO_2$ has not been demonstrated. Li_2CuO_2 adopts an orthorhombic structure,[14,15] whereas Li_2NiO_2 occurs in both rhombohedral and orthorhombic forms.[16]

The accommodation of additional Li into a host compound to form $P\bar{3}m1$ Li_2MO_2 without destruction of the rhombohedral symmetry would be expected to promote enhanced capacity and reversibility by avoiding a breakup of the layered host structure. In this article, we explore by first-principles calculations the energetics of such a reaction for several possible choices of M relative to other available reaction routes. A variety of reactions of Li with $LiMO_2$ are possible, in principle. The addition reaction

$$Li + LiMO_2 \rightarrow Li_2MO_2 \quad (1)$$

can result in either a layered rhombohedral or a nonlayered product compound Li_2MO_2. A second possibility is the decomposition of the ternary oxide into a monoxide MO (or possibly another oxide such as the sesquioxide M_2O_3, which, however, is not discussed in this article) and Li_2O

$$Li + LiMO_2 \rightarrow MO + Li_2O \quad (2)$$

A third possibility is the displacement reaction

$$3Li + LiMO_2 \rightarrow M + 2Li_2O \quad (3)$$

in which the metal M is extruded directly and lithia is formed. One cannot exclude the possibility of multiple reactions occurring simultaneously. Also, the displacement reaction can occur sequentially, with the decomposition reaction

* To whom correspondence should be addressed. E-mail: benedek@anl.gov.

(1) Delmas, C.; Fouassier, C.; Hagenmuller, P. *Phys. B* **1980**, *99*, 81.
(2) Tarascon, J. M.; Armand, M. *Nature* **2001**, *414*, 359.
(3) Ohzuku, T.; Makimura, Y. *Chem. Lett.* **2001**, *7*, 642.
(4) Ohzuku, T.; Makimura, Y. *Chem. Lett.* **2001**, *8*, 744.
(5) Koyama, Y.; Tanaka, I.; Adachi, H.; Makimura, Y.; Ohzuku, T. J. *J. Power Sources* **2003**, *119*−*121*, 644.
(6) Koyama, Y.; Makimura, Y.; Tanaka, I.; Adachi, H.; Ohzuku, T. *J. Electrochem. Soc.* **2004**, *151*, A1499.
(7) Koyama, Y.; Makimura, Y.; Tanaka, I.; Adachi, H.; Ohzuku, T. *J. Electrochem. Soc.* **2004**, *151*, A1545.
(8) Koyama, Y.; Makimura, Y.; Tanaka, I.; Adachi, H.; Ohzuku, T. *J. Electrochem.* **2005**, *73*, 2.
(9) Lu, Z.; MacNeil, D. D.; Dahn, J. R. *Electrochem. Solid-State Lett.* **2001**, *4*, A200.
(10) Johnson, C. S.; Kim, J. S.; Lefief, C.; Li, N.; Vaughey, J. T.; Thackeray, M. M. *Electrochem. Commun.* **2004**, *6*, 1085.
(11) Johnson, C. S.; Kim, J. S.; Kropf, A. J.; Kahaian, A. J.; Vaughey, J. T.; Fransson, L. M. L.; Edstrom, K.; Thackeray, M. M. *Chem. Mater.* **2003**, *15*, 2313.
(12) Vaughey, J. T.; Dawson, A.; Fackler, N.; Johnson, C. S.; Edstrom, K.; Bryngelsson, H.; Benedek, R.; Thackeray, M. M. **2006**, unpublished.
(13) David, W. I. F.; Goodenough, J. B.; Thackeray, M. M.; Thomas, M. G. S. R. *Rev. Chim. Miner.* **1983**, *20*, 636.
(14) Chung, E. M. L.; McIntire, G. J.; Paul, D. M.; Balakrishnan, G.; Lees, M. R. *Phys. Rev. B* **2003**, *68*, 144410.
(15) Vitins, G.; Raekelboom, E. A.; Weller, M. T.; Owen, J. R. *J. Power Sources* **2003**, *119*, 938.
(16) Davidson, I. J.; Greedan, J. E.; von Sacken, U.; Michal, C. A.; McKinnon, W. R. *J. Solid State Chem.* **1993**, *105*, 410.

10.1021/cm051854r CCC: $33.50
Published on Web 02/07/2006

preceding extrusion of *M* from *M*O by the reaction

$$2\mathrm{Li} + \mathrm{MO} \rightarrow \mathrm{M} + \mathrm{Li_2O} \quad (4)$$

The displacement reaction (eq 4) of transition-metal monoxides, with M = Co, Ni, and Fe, has been investigated.[17,18]

Because Li batteries operate at temperatures close to room temperature, there is generally little distinction between internal energy and free energy,[19] and only the former, which can readily be calculated with first-principles density functional theory methods,[19] is considered here. By calculating the energies of the reactant and product phases, we can predict the reaction energies, ΔE_r, for eqs 1−3.

Both thermodynamics and kinetics determine which reactions, or reaction sequences, actually occur in a given system and the extent of their reversibility. Thus, the reaction with the lowest ΔE_r does not necessarily occur if the kinetics are unfavorable. The displacement reaction, in which the transition-metal oxidation state is fully reduced in one step, apparently does not occur experimentally, despite having the smallest ΔE_r. Although the addition reaction is typically the least-favored energetically of eqs 1−3, it is observed experimentally for $M = Mn_{0.5}Ni_{0.5}$. The addition reaction has also been observed to occur, at least partially,[20] for M = Ni.The system M = Co, on the other hand, is found[12] to undergo the decomposition reaction.

The (absolute value of the) reaction energy (or free energy), ΔE_r, represents a thermodynamic upper limit to the open-circuit electrochemical cell voltage, V_0, measured during the first discharge cycle. In general, however, V_0 is often found to be considerably smaller than ΔE_r, particularly for the decomposition reaction. On the other hand, the fraction $V_0/\Delta E_r$ is much closer to unity for the addition reaction. It is reasonable to suggest that the more profound atomic rearrangements that occur during the reaction path for the decomposition result in a smaller value of $V_0/\Delta E_r$ for decomposition than for the addition reaction, for which only a modest change in crystal structure is required.

Method

The calculations presented in this article were performed with the VASP code,[21,22] which implements the local spin density functional approximation (LSDA) of density functional theory in a pseudopotential representation, with a plane wave basis. In particular, the GGA+U approximation is utilized, which combines the generalized gradient approximation (GGA) correction[23] to LSDA with the LSDA+U extension[24] of density functional theory. The GGA+U approximation in VASP is implemented within the projector augmented wave (PAW) formulation. It has been amply demonstrated that the GGA+U approximation affords greater accuracy for electronic and magnetic[25] as well as electrochemical properties,[26,27] relative to the LSDA-GGA, for insulating transition-metal oxides. The LSDA+U approximation accounts for the on-site Coulomb interaction by penalizing partial occupancy of atomic *d*-states on the transition-metal sublattice. A linear-response method to determine the optimal value of the Hubbard U parameter was recently proposed[28] and subsequently applied to several transition-metal compounds.[27] The numerical results of that work, as well as other calculations within the LSDA+U framework, suggest that, to a reasonable approximation

$$U_i = a_i + Z_i \quad (5)$$

where the transition metal i is in oxidation state Z_i and the constant a_i = 2 eV for Mn and a_i = 3 eV for Co and Ni. For simplicity, we adopt this parametrization in numerical calculations and set the exchange parameter J to 1 eV.[24] The variation of U with oxidation state implies a self-consistency condition. In the calculations, an initial guess is made for the oxidation state Z_i of ion M, which may need to be revised on the basis of the calculated results; if so, the calculation is then repeated with the value of U_i appropriate to Z_i. The oxidation state of a transition-metal ion is, in most instances, revealed by its bond length with nearest-neighbor oxygen ions.[29]

The explicit dependence of U on Z has mostly been ignored in previous LDA+U calculations; however, it seems more consistent to take this dependence into account when comparing systems in which Z takes on disparate values, as in the present work. We note, however, that calculations at the GGA level (results not presented here) of the properties considered in this article yield trends that are quite similar to those shown for GGA+U calculations.

Crystal Structures

A. Layered Systems. The atomic structure of compounds $LiMO_2$ with symmetry $R\bar{3}m$ (prototype α-$NaFeO_2$) can be described in terms of the *ABCABC* stacking of hexagonal layers, where successive Li and *M* layers are separated by O layers. Compounds with composition Li_2MO_2 may adopt either an orthorhombic[30] or a rhombohedral structure. The rhombohedral structure, for which the system Cu_2ErS_2 (or CdI_2) is the prototype, possesses symmetry $P\bar{3}m1$.[13] The corresponding stacking is

$$A_M B_O C_{Li} B_{Li} C_O \ldots \quad (6)$$

in which the anion layers follow a close-packed hexagonal arrangement, as opposed to the cubic arrangement for the

(17) Poizot, P.; Ruelle, S.; Grugeon, S.; Dupont, L.; Tarascon, J. M. *Nature* **2000**, *407*, 496.
(18) Dedryvere, R.; Laruelle, S.; Grugeon, S.; Poizot, P.; Gonbeau, D.; Tarascon, J. M. *Chem. Mater.* **2004**, *16*, 1056.
(19) Aydinol, M. K.; Kohan, A. F.; Ceder, G.; Cho, K.; Joannopoulos, J. *Phys. Rev. B* **1997**, *56*, 1354.
(20) Dahn, J. R.; von Sacken, U.; Michal, C. A. *Solid State Ionics* **1990**, *44*, 87.
(21) Kresse, G.; Furthmueller, J. *Comput. Mater. Sci.* **1996**, *6*, 15.
(22) Kresse, G.; Furthmueller, J. *Phys. Rev. B* **1996**, *54*, 11169.
(23) Wang, Y.; Perdew, J. P. *Phys. Rev. B* **1991**, *44*, 13298.
(24) Anisimov, V. I.; Zaanen, J.; Andersen, O. K. *Phys. Rev. B* **1991**, *44*, 943.
(25) Rohrbach, A.; Hafner, J.; Kresse, G. *J. Phys. Condens. Matter* **2003**, *15*, 979.
(26) Zhou, F.; Marianetti, C. A.; Cococcioni, C.; Morgan, G.; Ceder, G. *Phys. Rev. B* **2004**, *69*, 201101.
(27) Zhou, F.; Cococcioni, C.; Marianetti, C. A.; Morgan, G.; Ceder, G. *Phys. Rev. B* **2004**, *70*, 235121.
(28) Cococcioni, M.; de Gironcoli, S. *Phys. Rev. B* **2005**, *71*, 035105.
(29) Prasad, R.; Benedek, R.; Thackeray, M. M. *Phys. Rev. B* **2005**, *72*, 134111.
(30) Rieck, H.; Hoppe, R.; *Z. Anorg. Allg. Chem.* **1972**, *392*, 193.

$R\bar{3}m$ symmetry. The Li atoms occupy tetrahedral interstices rather than octahedral sites, as in LiMO$_2$.

The detailed reaction path by which the $R\bar{3}m$ structure of LiMO$_2$ transforms into the $P\bar{3}m1$ structure of Li$_2M$O$_2$ when the addition reaction occurs is unknown. In the most-direct transformation scheme, Li would first intercalate into the $R\bar{3}m$ structure to yield an intermediate structure with stacking

$$A_M B_O C_{Li} B_{Li} A_O B_M ... \quad (7)$$

in which the intercalation would presumably proceed via a process analogous to the Daumas−Herold picture of the staging of intercalation compounds[31] and result in a patchwork arrangement of columnar domains. In the intermediate structure, the inserted lithium layer (B_{Li}) is tetrahedrally coordinated, whereas the original Li layer (C_{Li}) is octahedrally coordinated. An unfavorable feature of this structure is that the inserted (B_{Li}) layer lies in registry with a nearby B_M layer (with an O layer sandwiched between them), so that some repulsive Li−M pairs possess short bond lengths of comparable in magnitude to M−O bond lengths, which does not occur in the $P\bar{3}m1$ structure.

One might expect that another unfavorable feature of the proposed intermediate structure would be the small Li−Li separations between the tetrahedrally coordinated (B_{Li}) and octahedrally coordinated (C_{Li}) layers. In fact, the Li−Li separations in the relaxed intermediate structures are approximately 2.50 Å, which is actually larger than the corresponding separations of about 2.35 Å in the relaxed $P\bar{3}m1$ structure. However, this is achieved by expanding the c-axis lattice constant, which results in an increase of the overall electrostatic energy.

For these reasons, the intermediate structure is energetically unfavorable, as demonstrated in the numerical calculations presented below. It would be unstable with respect to a transformation to the $P\bar{3}m1$ structure, which is stable. Such a transformation could perhaps occur via a martensitic process.

Although the proposed reaction path for the addition reaction, on the basis of Li intercalation followed by a martensitic transformation, appears plausible, no experimental evidence for it is presently available. Unlike the case of the multiphase reactions (eqs 2 and 3), however, phase separation accompanied by long-range diffusion is not required, and activation energies are therefore expected to be relatively low.

1. Transition-Metal Mixtures. We consider pseudobinary alloys with the composition Li$(M_1M_2)_{0.5}$O$_2$, in addition to the pure LiMO$_2$ systems. The ordering in LiMn$_{0.5}$Ni$_{0.5}$O$_2$ has been given the most attention in previous work; other pseudobinaries appear to have minimal, if any, ordering tendencies. The structure of the pseudobinary LiMn$_{0.5}$Ni$_{0.5}$O$_2$, which shows strong ordering tendencies, has previously[32−34] been investigated with first-principles and Monte Carlo methods. The calculations show that, in the absence of Li in the transition-metal layer, the low-energy structure of the transition-metal layers consists of alternating zigzag chains of Mn and Ni atoms (Figure 3a in Yoon et al.[32]). With Li present in the transition metal layer, a different configuration appears favorable.[33] In most of the calculations presented in this article, however, we employed an alternating straight-chain (or striped) arrangement (Figure 3b in Yoon et al.[32]), which has a smaller unit cell. Although the striped arrangement has a slightly higher energy than the zigzag structure, it suffices for illustrating the main trends.

2. Magnetic Structure. The magnetic structure of most layered systems is assumed to be ferromagnetic. Experiments on Ni-doped[35] LiMnO$_2$ and[36] LiNiO2 are consistent with this assumption; Co in LiCoO$_2$ is in a low-spin, essentially nonmagnetic configuration. We assume that doped LiMnO$_2$, which has a cooperative Jahn−Teller distortion, is characterized by antiferromagnetic chains along the close-packed b-axis.[37] We treat Li$_2M$O$_2$, with $P\bar{3}m1$ symmetry, as being ferromagnetic. Measurements[16] for Li$_2$NiO$_2$ show ferromagnetic layers with antiferromagnetic interlayer coupling. Although the magnetic structures assumed in our calculations are idealized, they are likely sufficiently close to the true structures to reproduce the correct trends for the properties of interest.

B. Monoxides. To evaluate the reaction energy for the decomposition reaction (eq 2), we require energies for the transition-metal monoxides. The calculations for MnO, NiO, and CoO are made on the basis of the same assumed structure, rhombohedrally distorted rock salt, with AFII antiferromagnetic order,[38] in which close-packed (111) transition-metal layers are ferromagnetic and adjacent layers have opposite spin. In the case of CoO, a tetragonal structure was observed[39] at temperatures less than about 200 K but was not addressed in this work.

C. Metals. To evaluate the reaction energy for the displacement reaction (eq 3), we require cohesive energies for the pure transition metals Mn, Co, and Ni. Ferromagnetic Co is hexagonal,[39] and ferromagnetic Ni is face-centered cubic.[39] The 58-atom cubic unit cell[40] of α-Mn was employed in calculations for metallic Mn. The magnetic structure of α-Mn is complex. To obtain an energy for Mn, we first calculated an E_{nonmag} value for the system without spin polarization. A detailed investigation of the ground-state magnetic structure[40] (on the basis of a different exchange-correlation functional) yielded an energy $\Delta E_{mag} \approx 0.1$ eV per atom less than that for nonmagnetic α-Mn. In reaction energy calculations, we employ an energy $E = E_{nonmag} - \Delta E_{mag}$ for Mn. This may be regarded as a lower bound, because a chemical reaction at room temperature most likely

(31) Daumas, N.; Herold, A.; *C. R. Seances Acad. Sci., Ser. C*. **1969**, *268*, 373.
(32) Yoon, W. S.; Iannopollo, S.; Grey, C. P.; Carlier, D.; Gorman, J.; Reed, J.; Ceder, G. *Electrochem. Solid-State Lett.* **2004**, *7*, A167.
(33) Van der Ven, A.; Ceder, G. *Electrochem. Commun.* **2004**, *6*, 1045.
(34) Meng, Y. S.; Ceder, G.; Grey, C. P.; Yoon, W. S.; Jiang, M.; Breger, J.; Shao-Horn, Y. *Chem. Mater.* **2005**, *17*, 2386.
(35) Spahr, M. E.; Novak, P.; Schnyder, B.; Haas, O.; Nesper, R. *J. Electrochem. Soc.* **1998**, *145*, 1113.
(36) Hewston, T. A.; Chamberland, B. L. *J. Phys. Chem. Solids* **1987**, *48*, 47.
(37) Singh, D. *Phys. Rev. B* **1997**, *55*, 309.
(38) Pask, J. E.; Singh, D. J.; Mazin, I. I.; Hellberg, C. S.; Kortus, J. *Phys. Rev. B* **2001**, *64*, 024403.
(39) Villars, P.; Calvert, L. D. *Pearson's Handbook of Crystallographic Data for Intermetallic Phases*; ASM International: Materials Park, OH, 1991.
(40) Hobbs, D.; Hafner, J.; Spisak, D. *Phys. Rev. B* **2003**, *68*, 014407.

Table 1. Structural Parameters for $LiMO_2$[a]

M	theory or expt	*a*	*b*	*c*	$R(M_1-O)$	$R(M_2-O)$
Mn	theory	5.51	2.85	5.42	1.96, 2.34	
Mn	expt[48,49]	5.438	2.808	5.387		
Ni	theory	2.89		14.33	1.98	
Ni	expt[36]	2.88		14.19		
Co	theory	2.83		14.18	1.94	
Co	expt[50]	2.82		14.04		
$Mn_{0.5}Ni_{0.5}$	t(striped)	2.93		14.48	1.96	2.07
$Mn_{0.5}Ni_{0.5}$	t(zigzag)	2.89		14.23	1.94	2.05
$Mn_{0.5}Ni_{0.5}$	expt[11]	2.88		14.28		
$Mn_{0.5}Co_{0.5}$	theory	2.96		14.48	1.97	2.09
$Ni_{0.5}Co_{0.5}$	theory	2.91		14.46		2.02
$Ni_{0.5}Co_{0.5}$	expt[45,51]	2.85		14.13		

[a] Monoclinic structure (symmetry *C*2/*m*) assumed for M = Mn; results for the other systems correspond to the rhombohedral structure (symmetry $R\bar{3}m$). Lattice constants, *a*, *b*, and *c*, and M−O bond lengths $R(M_1-O)$ and $R(M_2-O)$, where M_1 is Mn and M_2 is Ni in the case of $Mn_{0.5}Ni_{0.5}$, and similarly for $Mn_{0.5}Co_{0.5}$ and $Ni_{0.5}Co_{0.5}$, are in Å.

Table 2. Compound Formation Energies (eq 8, in eV per formula unit) for Pseudobinary Alloys $Li(M_1M_2)_{0.5}O_2$[a]

M	theory or expt	structure	ΔH_m
$Mn_{0.5}Ni_{0.5}$	GGA	striped	−0.19
$Mn_{0.5}Ni_{0.5}$	GGA+U	striped	−0.03
$Mn_{0.5}Ni_{0.5}$	GGA+U	zigzag	−0.15
$Mn_{0.5}Co_{0.5}$	GGA	striped	0.24
$Mn_{0.5}Co_{0.5}$	GGA+U	striped	0.01
$Ni_{0.5}Co_{0.5}$	GGA	striped	−0.02
$Ni_{0.5}Co_{0.5}$	GGA+U	striped	0.11
$Ni_{0.5}Co_{0.5}$	expt[45]		0.02

[a] Monoclinic structure (symmetry *C*2/*m*) assumed for M = Mn; results for the other systems correspond to the rhombohedral structure (symmetry $R\bar{3}m$). The experimental value for $Ni_{0.5}Co_{0.5}$ is a heat of mixing determined by calorimetry.

would not yield a crystal structure as complex as that of α-Mn.

We employ the GGA method, equivalent to setting $U - J = 0$, instead of the standard GGA+U scheme in calculations for the metallic systems, for which it is not well-suited.[41]

Results

A. Atomic Structure. Calculations were performed to determine the reaction energies for the addition, decomposition, and displacement reactions (eqs 1−3) for compounds Li_xMO_2, with *M* = Co, Mn, and Ni, as well as for the pseudobinaries *M* = $Co_{0.5}Mn_{0.5}$, $Co_{0.5}Ni_{0.5}$, and $Mn_{0.5}Ni_{0.5}$. To evaluate the reaction energies, we require the energies of the corresponding reactants and products.

The striped structure is employed in most of the calculations for pseudobinary systems, as noted above. The internal coordinates as well as the lattice constants are relaxed in each system, to minimize the energy, whereas the lattice vectors are constrained to be consistent with trigonal symmetry.

Calculated equilibrium lattice constants and bond lengths are listed Tables 1 and 3−5. Comparison of the predicted lattice constants with experimental values is a test of the reliability of the methods employed in this work, namely GGA+U for the oxides and GGA for the pure metals. The lattice constants are typically slightly overestimated by these methods, relative to experimental values. Compound formation energies ΔH_f are listed in Table 2.

Table 3. Structural Parameters for Li_2MO_2 in Rhombohedral Structure ($P\bar{3}m1$)[a]

M	theory or expt	*a*	*c*	$R(M_1-O)$	$R(M_2-O)$
Mn	theory	3.21	5.34	2.27	
Mn	expt[13]	3.195	5.303		
Ni	theory	3.13	5.06	2.16	
Ni	expt[16]	3.095	5.070		
Co	theory	3.14	5.16	2.19	
$Mn_{0.5}Ni_{0.5}$	t(striped)	3.16	5.20	2.24	2.19
$Mn_{0.5}Ni_{0.5}$	t(zigzag)	3.16	5.27	2.24	2.19
$Mn_{0.5}Ni_{0.5}$	expt[11]	3.13	5.196		
$Mn_{0.5}Co_{0.5}$	theory	3.18	5.13	2.26	2.21
$Ni_{0.5}Co_{0.5}$	theory	3.13	5.13	2.17	2.18

[a] Lattice constants and M−O bond lengths $R(M_1\text{-O})$ and $R(M_2\text{-O})$ where M_1 is Mn and M_2 is Ni in the case of $Mn_{0.5}Ni_{0.5}$, and similarly for $Mn_{0.5}Co_{0.5}$ and $Ni_{0.5}Co_{0.5}$, are in Å. In the case of $Mn_{0.5}Ni_{0.5}$, calculations are performed for striped and zigzag ordered arrangements in the transition-metal layers.

Table 4. Structural Parameters for *M*O in Rhombohedral Structure (rocksalt with trigonal distortion)[a]

M	theory or expt	*a*	$\Delta\phi$	$R(M-O)$
Mn	theory	4.48	0.77	2.24
Mn	expt[52]	4.43	0.62	
Ni	theory	4.20	0.47	2.10
Ni	expt[39]	4.17		
Co	theory	4.28	0.86	2.14
Co	expt[39]	4.26		

[a] Adjacent close-packed *M* layers are assumed to have opposite spin. $\Delta\phi$ represents a deviation of the angle between trigonal axes from 90 degrees.

Table 5. Structural Parameters for Metals[a]

M	theory or expt	*a*	*c*
Mn	theory	8.55	
Mn	expt	8.91	
Ni	theory	3.49	
Ni	expt	3.51	
Co	theory	2.49	4.01
Co	expt	2.505	4.069

[a] Lattice parameters in Å. Calculation for α-Mn assumes a nonmagnetic system.

Previous calculations for the pseudobinary systems under consideration were performed within the local spin density approximation (LSDA) by Koyama et al.[6] The present work and that of Koyama et al. agree qualitatively in showing formation energies for $Mn_{0.5}Ni_{0.5}$ to be more negative than those of the other two equiatomic pseudobinaries, *M* = $Co_{0.5}$-$Mn_{0.5}$ and $Co_{0.5}Ni_{0.5}$. The absolute values of the predicted lattice constants and ΔH_f in the present work, however, differ somewhat from the previous calculations,[6] because of the different approximations to electron exchange and correlation employed.

1. Lattice Constants. Results for $LiMnO_2$ in Table 1 correspond to the layered monoclinic structure. In the case of *M* = $Mn_{0.5}Ni_{0.5}$, the calculated lattice constants for the zigzag structure, which is favored energetically,[32] are in slightly better agreement with experimental values[11] than are those for the striped structure. In the case of Ni, the calculation is done for the experimentally observed $R\bar{3}m$ structure, although Ni^{3+} is known to adopt a low-spin Jahn−Teller active configuration.[42] We are not aware of measured lattice constants for equiatomic alloys of Mn and Co,

(41) Petukhov, A. G.; Mazin, I. I. *Phys. Rev. B* **2003**, *67*, 153106.

although measurements[43] have been made for Mn-rich compositions of this system. Vegard's law behavior has been observed experimentally[44] for the crystallographic parameters of $LiNi_{1-y}Co_yO_2$, but clustering tendencies were evident in EPR measurements. The calculations for striped layers of $LiNi_{0.5}Co_{0.5}O_2$ are discussed below. In addition to the calculations for the striped structure, two other structures were considered for $LiNi_{0.5}Co_{0.5}O_2$. In one of them, we assume an alternation of pure Ni and Co layers along the *c*-axis, and in the other, a nominally disordered arrangement of Co and Ni atoms in a 16-atom per layer unit cell. In the alternating layer arrangement, our cell relaxation procedure was unable to achieve low stresses without breaking the rhombohedral symmetry of the unit-cell vectors. In the nominally disordered arrangement (8 Ni and 8 Co atoms are distributed more or less randomly in the transition-metal layer), we were unable to obtain a stable relaxed atomic configuration, because of charge fluctuations during the relaxation process. These calculations, as well as the heat of mixing analysis described below, suggest that $Ni_{0.5}Co_{0.5}$ may exhibit Ni and Co clustering and therefore be difficult to synthesize as microscopically homogeneous alloys.

Calculated compound formation energies

$$\Delta H_f = E_{(Li(M_1M_2)0.5O_2)} - [E_{(LiM_1O_2)} + E_{(LiM_2O_2)}]/2 \quad (8)$$

are listed in Table 2. $Mn_{0.5}Ni_{0.5}$ shows a negative value of ΔH_f, consistent with the strong ordering tendency of this system.[32,34] The zigzag structure, as expected, shows a lower formation energy than the striped structure. The other pseudobinaries show ΔH_f values for the striped structure that are either positive or close to zero. Table 2 lists results of GGA as well as GGA+U calculations. The GGA calculations (and previous LSDA calculations[6]), exhibit values of ΔH_f different from those of the GGA+U method, but all of these treatments show ordering tendencies of $Mn_{0.5}Ni_{0.5}$. Overall, we would expect predictions of the GGA+U methods to be slightly more realistic than those of the lower-level methods.

In the case of $Ni_{0.5}Co_{0.5}$, the GGA+U prediction of a large positive ΔH_f suggests that ordering (or mixing) is unfavorable, which is consistent with the experimental observation of clustering.[44] Furthermore, a calorimetric determination of the heat of mixing[45] for $Ni_{0.5}Co_{0.5}$ is well below the GGA+U calculation of ΔH_f, which suggests that the experiment represents a much more clustered state for this system than for the striped structure. Table 2 lists lattice constants for the overlithiated compound Li_2MO_2. As in the case of $LiMO_2$, calculated lattice parameters agree closely with experimental values, where available. Table 3 lists results for the monoxides of Mn, Co, and Ni. Calculated results are in close agreement with experimental values. Results for the pure metals are given in Table 4. Agreement of the present calculations with experimental values is worse for Mn; however, agreement is improved when a non-collinear magnetic state[40] is considered.

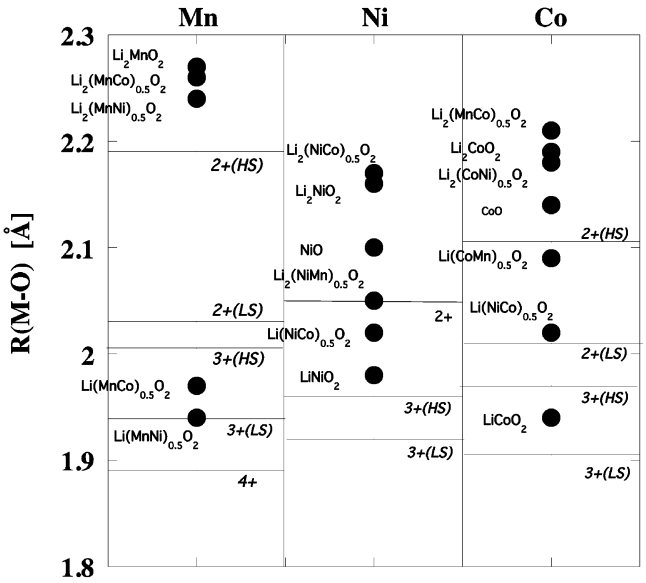

Figure 1. Calculated cation−oxygen bond lengths in $LiMO_2$. Circles represent results for the indicated compounds. Lines represent the sum of the ionic radii[47] for the octahedrally coordinated cation indicated and for divalent oxygen. The bond length for $LiMnO_2$ is omitted because of the large Jahn−Teller distortion; cf. Table 1.

2. Metal−Oxygen Bond Lengths and Oxidation States. For convenience, we frame our discussion of transition-metal oxidation states in terms of the calculated metal−oxygen bond lengths,[29] although the relationship between bond length and oxidation state is complicated by the fact that oxygen is not necessarily divalent in all of the systems under consideration.[19,46]

Results for transition metal−oxygen bond lengths calculated for the oxides treated in this work are plotted in Figure 1 as filled circles (the plotted value is the mean bond length when the octahedron is distorted). For comparison, the horizontal lines indicate the sum of ionic radii,[47] $R(M^{Z+}) + R(O^{2-})$, of octahedrally coordinated Mn, Ni, and Co, in various oxidation states, and an oxygen ion. The radius for oxygen was taken to be 1.36 Å, appropriate for a coordination number of 3. For most of the cases considered, the bond length calculated by first principles is slightly higher than the sum of the ionic radii for the appropriate oxidation states.

For $LiMn_{0.5}Ni_{0.5}O_2$ and $LiMn_{0.5}Co_{0.5}O_2$, the calculations suggest that Mn is quadrivalent and Ni or Co divalent; this assignment is confirmed by examination of the local density of electronic states (not shown here). In the case of $LiCo_{0.5}Ni_{0.5}O_2$, however, Ni exhibits a strong Jahn−Teller distortion, and both Ni and Co appear trivalent. In $LiCo_{0.5}Ni_{0.5}O_2$, with the striped ordering of cations, the Jahn−Teller activity of Ni introduces shear stresses that cannot be removed by relaxation without destroying the rhombohedral symmetry.

(42) Marianetti, A.; Morgan, D.; Ceder, G. *Phys. Rev. B* **2004**, *63*, 224304.
(43) Armstrong, A. R.; Robertson, A. D.; Bruce, P. G. *Electrochim. Acta* **1999**, *45*, 285.
(44) Zhecheva, E.; Stoyanova, R.; Alcantara, R.; Lavela, P.; Tirado, J. L. *Pure Appl. Chem.* **2002**, *74*, 1885.
(45) Wang, M.; Navrotsky, A. *Solid State Ionics* **2004**, *166*, 167.
(46) Montoro, L. A.; Abbate, M.; Almeida, E. C.; Rosolen, J. M. *Chem. Phys. Lett.* **1999**, *309*, 14.
(47) Shannon, R. D. *Acta Crystallogr.* **1976**, *32*, 751.
(48) Armstrong, A. R.; Bruce, P. G. *Nature* **1996**, *381*, 499.
(49) Capitaine, F.; Gravereau, P.; Delmas, C. *Solid State Ionics* **1996**, *89*, 197.
(50) Ohzuku, T.; Ueda, A.; Nagayama, M.; Iwakoshi, Y.; Komori, H. *Electrochim. Acta* **1993**, *38*, 1159.
(51) Castro-Garcia, S.; Castro-Coucieiro, A.; Senaris-Rodriguez, M. A.; Soulette, F.; Julien, C. *Solid State Ionics* **2003**, *156*, 15.
(52) Shaked, H.; Faber, J.; Hitterman, R. L. *Phys. Rev. B* **1988**, *38*, 11901.

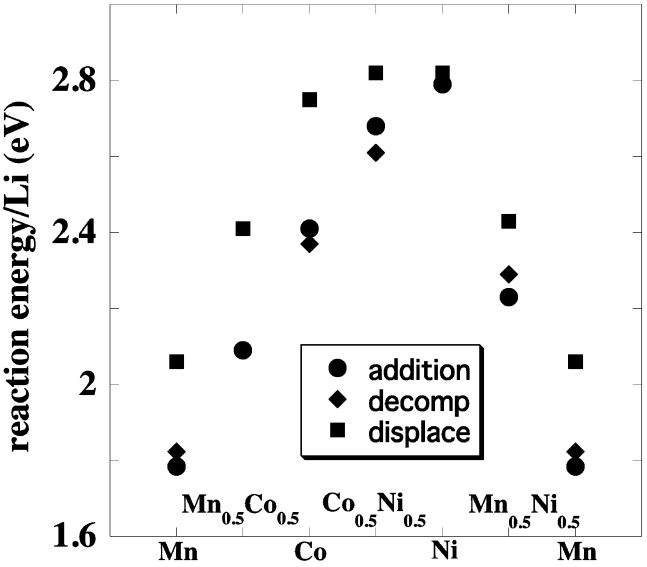

Figure 2. Reaction energies, ΔE_r, per Li atom for Li with $LiMO_2$. Results are shown for the addition, decomposition, and displacement reactions, defined in eqs 1−3. In the case of $Mn_{0.5}Ni_{0.5}$, the addition and decomposition reaction energies are essentially identical.

In the overlithiated systems with composition Li_2MO_2, with either a single component or an ordered binary arrangement on the *M* sublattice, Mn, Co, and Ni are all divalent, with bond lengths slightly longer than those in rhombohedral monoxides *M*O.

B. Intermediate State. As a complement to our calculations for the equilibrium phases, we also treated the proposed intermediate states described in section III, which may be relevant to the reaction path for the addition reaction. For the systems with composition Li_2MO_2, including both single component and pseudobinaries, the intermediate state energy was approximately 0.75 eV per formula unit higher than that for the equilibrium ($P\bar{3}m1$) structure.

We note, however, that in the case of Li_2CoO_2, the energy of the intermediate structure was several tenths of an eV higher unless symmetry is broken by a small displacement of the Co atoms. Without this displacement, the d-electron density of electronic states is ungapped at the Fermi energy, but a gap is introduced when the Co atom displacement occurs. For Mn in the 4+ and Ni in the 2+ oxidation states, however, the e_g and t_{2g} multiplets are either filled or empty as a result of crystal-field splitting, and a gap is present without any further symmetry breaking. The larger energy barrier (in the absence of symmetry breaking) to overlithiating $LiCoO_2$ compared to that for the other $R\bar{3}m$ systems may be an additional factor that makes an addition reaction unfavorable for $LiCoO_2$.

C. Reaction Energies. Energies were calculated for the addition, decomposition, and displacement reactions (eqs 1−3) for compounds Li_xMO_2, with M = Co, Mn, and Ni, as well as for pseudobinaries $M = Co_{0.5}Mn_{0.5}$, $Co_{0.5}Ni_{0.5}$, and $Mn_{0.5}Ni_{0.5}$. Results are plotted in Figure 2 for the reaction energy, in eV, per reacting Li. As expected, the reaction energies for the pseudobinaries are close to the averages of the single-component results for their constituents ($\Delta E_r(Mn_{0.5}Ni_{0.5}) \approx (\Delta E_r(Mn) + \Delta E_r(Ni))/2$, where *E* denotes the addition, decomposition, or displacement energy). Of the systems considered, the highest reaction energies occur for Ni, which is consistent with the trend of higher ionization energies for later transition metals.

The displacement reaction, eq 3, in which the transition elements are reduced to their metallic state, is in all cases more favorable energetically than the reactions given in eqs 1 and 2. (For the purpose of this analysis, the product states for the pseudobinary systems in the case of decomposition and displacement reactions are assumed to be fully dissociated, e.g., MnO and NiO or Mn and Ni metal.) That the displacement reaction does not occur directly, for example, in the case of $Mn_{0.5}Ni_{0.5}$, is most likely because the energetically preferred reaction is blocked by kinetic barriers.

Of the systems considered, the only one for which an addition reaction has been observed[11] is $Li_xMn_{0.5}Ni_{0.5}O_2$. Ideally, the predicted reaction energy would be equal to the electrochemical cell voltage, in which Li metal is the counter electrode. The measured cell voltage[11] for $LiMn_{0.5}Ni_{0.5}O_2$, however, is about 1.8 eV, somewhat lower than the predicted reaction energy (for the addition reaction with the $P\bar{3}m1$ $Li_2Mn_{0.5}Ni_{0.5}O_2$ as the product) of 2.25 eV. A possible explanation for the discrepancy is that the measured cell voltage is determined not (or not only) by the equilibrium structure with symmetry $P\bar{3}m1$ but by some intermediate structure as well. The idealized intermediate structure postulated in this work, with an energy about 0.75 eV above that of the $P\bar{3}m1$ structure, would have a reaction energy of approximately 1.5 eV. We reiterate, however, that there is no direct evidence for the intermediate structure proposed in this work.

Discussion and Conclusions

We have applied first-principles methods to calculate the energies ΔE_r for the reaction of Li with several layered compounds of composition $LiMO_2$. The results exhibit the following trends. Absolute values of ΔE_r scale with the atomic number of *M* and increase through the series Mn, Co, Ni. In most cases (M = Ni is the exception), ΔE_r is far larger (by more than 0.1 eV per reacting Li) for the displacement reaction than for the addition or decomposition reactions. The addition and decomposition reaction energies, on the other hand, are comparable and differ by only hundredths of an eV, with decomposition typically slightly preferred. Only the addition (e.g., for $M = Mn_{0.5}Ni_{0.5}$) and decomposition reactions (e.g., for M = Co) appear to be observed experimentally. It is possible, and perhaps likely, that the selection of one or the other of these two reaction types is kinetically driven. For example, the decomposition reaction energy is lower even for $M = Mn_{0.5}Ni_{0.5}$, for which the addition reaction is observed experimentally. We note, however, that for ΔE_r differences as small as they are between the addition and decomposition reactions, entropic contributions to the free energy, which we have ignored, may be relevant. The nonobservation of the displacement reaction may more unambiguously be attributed to high activation barriers.

ΔE_r represents a thermodynamical upper limit to the (open-circuit) voltage V_0 of an electrochemical cell in which Li metal and $LiMO_2$ are the electrodes, and thus $v \equiv V_0/\Delta E_r \leq$

1. The measured voltage for the addition reaction in the case of $M = Mn_{0.5}Ni_{0.5}$ is about 1.8 eV, whereas the calculated E_r is 2.25 eV, so that $\upsilon \approx 0.8$. In the case of simple intercalation processes that are highly reversible (such as the addition of Li to Li_xCoO2, $x < 1$), υ may differ only minimally from unity.[27] The addition reaction (eq 1), however, is accompanied by a structural change from $R\bar{3}m$ to $P\bar{3}m1$ symmetry, which is expected to lessen the reversibility of the reaction and result in a less-than-ideal value of υ. The reaction path for the decomposition reaction (eq 2) involves more extensive atomic rearrangement than the addition reaction and therefore greater irreversibility and a lower value of υ. For $M = Co$, a voltage $V \approx 0.6$ eV, which corresponds to $\upsilon \approx 0.25$, was measured[12] for the decomposition reaction, albeit not under open circuit conditions.

Acknowledgment. This work was supported at Argonne National Laboratory by the Office of FreedomCar and Vehicle Technologies (Batteries for Advanced Transportation Technologies (BATT) Program), U.S. Department of Energy, under Contract W31-109-Eng-38. Grants of computer time at the National Energy Research Supercomputer Center, Lawrence Berkeley Laboratory, and at the JAZZ cluster, Argonne National Laboratory, are gratefully acknowledged.

CM051854R